Draft version April 14, 2015
Preprint typeset using LaTeX style emulateapj v. 12/16/11

BINARY ASTROMETRIC MICROLENSING WITH GAIA

Sedighe Sajadian [1,2]

Draft version April 14, 2015

Abstract

We investigate whether Gaia can specify the binary fractions of massive stellar populations in the Galactic disk through astrometric microlensing. Furthermore, we study if some information about their mass distributions can be inferred via this method. In this regard, we simulate the binary astrometric microlensing events due to massive stellar populations according to the Gaia observing strategy by considering (i) stellar-mass black holes, (ii) neutron stars, (iii) white dwarfs and (iv) main-sequence stars as microlenses. The Gaia efficiency for detecting the binary signatures in binary astrometric microlensing events is $\sim 10-20$ per cent. By calculating the optical depth due to the mentioned stellar populations, the number of the binary astrometric microlensing events being observed with Gaia with detectable binary signatures, for the binary fraction about 0.1, is estimated as 6, 11, 77 and 1316 respectively. Consequently, Gaia can potentially specify the binary fractions of these massive stellar populations. However, the binary fraction of black holes measured with this method has the large uncertainty owing to a low number of the estimated events. Knowing the binary fractions in massive stellar populations helps for studying the gravitational waves. Moreover, we investigate the number of massive microlenses which Gaia specifies their masses through astrometric microlensing of single lenses toward the Galactic bulge. The resulted efficiencies of measuring the mass of mentioned populations are 9.8, 2.9, 1.2 and 0.8 per cent respectively. The number of their astrometric microlensing events being observed in the Gaia era in which the lens mass can be inferred with the relative error less than 0.5 toward the Galactic bulge is estimated as 45, 34, 76 and 786 respectively. Hence, Gaia potentially gives us some information about the mass distribution of these massive stellar populations.

Keywords: Gravitational lensing: micro - Astrometry- Stars: binaries: general- methods: numerical

1. INTRODUCTION

Gaia is a space observatory of the European Space Agency (ESA), performing high precision astrometry, multi-colour, multi-epoch photometry and spectroscopy on astronomical objects brighter than 20 G magnitudes. This satellite, surveying the throughout sky, will observe each object 72 times averagely during five years of its lifetime (Eyer et al. 2013). The astrometric precision of Gaia depends strongly on the source magnitude and will be 30μas to 600μas for a single astrometric measurement of stars with magnitude 13 to 19 (Varadi et al. 2009). Different astronomical phenomena could be observed during the Gaia mission, e.g. supernovae (Belokurov & Evans 2003), novae, dwarf novae, eruptive stars, variable stars (Varadi et al. 2009; Eyer et al. 2013), astrometric microlensing events (Belokurov & Evans 2002; Proft et al. 2011), etc. Here, we study some features of detecting the last one with Gaia.

If the light of a background star passes through the gravitation field of a collinear foreground object, according to the Einstein general relativity, the light beam bends toward the center of gravity (Einstein 1936). Consequently, several distorted, (un)magnified images are produced whose angular separations are too small to be resolved even by modern telescopes. Instead, the combined and magnified light of images is received by observer, so-called gravitational microlensing. One of its feature is the displacement between the light centroid of images and the source position while the source star is passing the gravitational field of lens, i.e. astrometric trajectory (Walker 1995; Miyamoto & Yoshii 1995; Høg et al. 1995; Jeong et al. 1999). During a microlensing event by measuring the astrometric lensing and parallax effect, the mass of the deflector can be inferred (Paczyński 1998; Miralda-Escudé 1996). In microlensing events, the astrometric cross-section is much larger than the photometric one (Paczyński 1996). Hence, the optical depth of astrometric microlensing events is larger than the photometric one (Dominik & Sahu 2000).

Detecting the astrometric microlensing with the Gaia satellite was first discussed by Dominik & Sahu (2000). Then, Belokurov and Evans (2002) studied this subject by more details.The astrometric microlensing due to massive objects in solar orbit beyond the Kuiper Belt was investigated by Gaudi and Bloom (2005). Also, Proft et al. (2011) investigated several catalogs to find several nearby stars with large proper motions which are potential candidates for the astrometric microlensing detection in the Gaia era.

Here, we investigate quantitatively the Gaia efficiency for specifying the *binarity fractions of microlenses* in binary astrometric microlensing due to massive stellar populations, i.e. stellar-mass black holes, neutron stars and white dwarfs in addition to main-sequence stars. In order to obtain the Gaia efficiency, we preform a Monte Carlo simulation. Then, we evaluate the optical depth

sajadian@ipm.ir
[1] School of Astronomy, Institute for Research in Fundamental Sciences (IPM), P.O. Box 19395-5531, Tehran, Iran
[2] Department of Physics, Sharif University of Technology, P.O. Box 11155-9161, Tehran, Iran

and the number of binary events being observed with Gaia with detectable binary signatures, considering different binary fractions for massive stellar populations. Indicating the binary fractions in massive stellar populations is useful for studying the gravitational waves and estimating their amounts, see e.g. Riles (2013), Cutler and Thorne (2002). We find that Gaia can potentially point out the binary fractions of massive stellar populations. Furthermore, we estimate the Gaia efficiency for measuring the mass of *massive* stellar populations in the Galactic disk through astrometric microlensing of a single lens to indicate if Gaia can give any information about their mass distributions. Indeed, astrometric microlensing events due to more massive microlenses have longer Einstein crossing times and larger angular Einstein radii. Therefore, the Gaia efficiency for measuring the lens mass in these events is high.

This paper is organized as follows: In section (2) the basics of astrometric microlensing are explained. In the next section, we simulate binary astrometric microlensing events being observed with Gaia to investigate how much information Gaia gives us about the binary stellar populations in the Galactic disk. In section (4) we study if Gaia can determine the mass distributions of massive stellar populations through detecting astrometric microlensing of a single lens. We conclude in the last section.

2. BASICS OF ASTROMETRIC MICROLENSING

In microlensing events, the light centroid vector of source star images does not coincide with the source position. This astrometric shift in source star position changes with time as a microlensing event progresses. For a point-mass lens, the centroid shift vector of source star images is given by (Walker 1995; Miyamoto & Yoshii 1995; Høg et al. 1995):

$$\delta\theta_c = \frac{\mu_1\theta_1 + \mu_2\theta_2}{\mu_1+\mu_2} - \mathbf{u}\theta_E = \frac{\theta_E}{u^2+2}\mathbf{u}, \qquad (1)$$

where θ_i and μ_i are the position and magnification factor of ith image, $\mathbf{u} = p\hat{x} + u_0\hat{y}$ is the vector of the projected angular position of the source star with respect to the lens normalized by the angular Einstein radius of the lens θ_E in which $p = (t-t_0)/t_E$, t_0 is the time of the closest approach, t_E is the Einstein crossing time, $\hat{x}$ and $\hat{y}$ are the unit vectors in the directions parallel with and normal to the direction of the lens-source transverse motion. The angular Einstein radius of lens is given by:

$$\theta_E = \sqrt{\kappa\ M_l\ \pi_{rel}} = 300\mu as\sqrt{\frac{M_l}{0.3M_\odot}}\sqrt{\frac{\pi_{rel}(mas)}{0.036}}, (2)$$

where M_l is the lens mass, $\kappa = 4G/(c^2 A.U.)$ and $\pi_{rel} = A.U.(\frac{1}{D_l} - \frac{1}{D_s})$ where D_l and D_s are the lens and source distances from the observer. Usually, a microlensing parallax is defined as $\pi_E = \pi_{rel}/\theta_E$ which can be measured from the photometric event. According to equation (2), by measuring the relative parallax π_{rel} and the angular Einstein radius from astrometric observations the lens mass can be inferred. Nearby lenses have considerable and measurable relative parallaxes and the angular Einstein radii which are suitable candidates for astrometric measurements with Gaia. In that case, if the lens mass is high, the error bars of the lenses mass strongly decrease due to their large angular Einstein radii.

In astrometric microlensing, the threshold amount of impact parameter i.e. u_a which gives an astrometric centroid shift more than a threshold amount i.e. δ_T is given by:

$$u_a = \sqrt{\frac{T_{obs}v_t}{\delta_T D_l}} = 25.4\sqrt{\frac{T_{obs}(yr)}{5}}\sqrt{\frac{5\sqrt{2}\sigma_a}{\delta_T}} \times \\ \times\sqrt{\frac{v_t(km/s)}{130}}\sqrt{\frac{0.1}{D_l(Kp)}}, \qquad (3)$$

where T_{obs} is the lifetime of the satellite and v_t is the relative velocity of source with respect to the lens (Dominik & Sahu 2000). Here, we assume that the astrometric centroid shifts more than $\delta_T = 5\sqrt{2}\sigma_a$ are measurable with Gaia in which σ_a is the Gaia astrometric precision. Since Gaia can measure the astrometric displacement only along the scan, we combine σ_a with a factor of $\sqrt{2}$ to give the Gaia two-dimensional accuracy (Belokurov & Evans 2002). The amount of the threshold impact parameter for a typical astrometric microlensing event being observed with Gaia with the astrometric precision $\sigma_a = 300\ \mu as$ is equal to $u_a \sim 25$ whereas the threshold impact parameter for the photometric observation of a microlensing event is about one. Hence, the astrometric cross-section which is proportional to $\propto u_a^2$ is much larger than the photometric one.

2.1. *Astrometric optical depth*

According to the definition of the threshold impact parameter u_a, during the observational time T_{obs} the effective area around each lens which yields an astrometric shift in the projected source positions more than the threshold amount δ_T is $\mathcal{A}(x, M_l) = 2u_a R_E T_{obs} v_t$. This area is a function of the lens mass M_l and the lens distance $D_l = xD_s$ from the observer. The astrometric optical depth is defined as the cumulative fraction of these areas in the lens plane, for all lens distances from the observer to the source star which is given by (Dominik & Sahu 2000):

$$\tau_a = D_s\int_0^1 dx\rho_d(x)\int_0^\infty dM_l\frac{f(M_l)}{M_l}\mathcal{A}(x, M_l), \qquad (4)$$

where $f(M_l)$ is the distribution function of the lens mass and $\rho_d(x)$ is the stellar density distribution in the Galactic disk. We use the following distribution for the Galactic disk(Rahal et al. 2009):

$$\rho_d(x) = \frac{\Sigma}{2H}\exp(\frac{-(R-R_\odot)}{h})\exp(\frac{-|z|}{H}), \qquad (5)$$

where R is the radial distance from the Galactic center, z is the altitude with respect to the Galactic plane, $H = 0.325\ kpc$ is the height scale, $h = 3.5\ kpc$ is the length scale of the disk and Σ is the column density of the disk at the Sun position. By inserting the amount of $\mathcal{A}(x, M_l)$,

the optical depth is:

$$\tau_a = 4\sqrt{\frac{G}{c^2}} D_s \sqrt{\frac{T_{obs}^3 v_t^3}{5\sqrt{2}\sigma_a}} \int_0^1 dx \;\; \rho_d(x)\sqrt{1-x} \int_0^\infty dM_l \, \frac{f(M_l)}{\sqrt{M_l}}. \quad (6)$$

The optical depth can be used to estimate the number of observed events. If N_{bg} background source stars brighter than 20 G magnitudes are observed during the Gaia lifetime T_{obs}, the number of source stars with the astrometric shift, in their projected positions, more than δ_T is given by:

$$N_a = \frac{\pi}{2} \frac{T_{obs} N_{bg}}{t_E u_a} \tau_a. \quad (7)$$

By considering ε as the efficiency for measuring the lens mass of these observed events, the number of astrometric microlensing events being observed with Gaia in which the lens mass can be measured is $N_e = N_a \, \varepsilon$.

3. BINARY ASTROMETRIC MICROLENSING DURING THE GAIA MISSION

The binary fractions of massive stellar populations have not explicitly been specified yet. However, this issue is very important for studying the gravitational waves. Because, the sources of the gravitational waves are binary systems composed of white dwarfs, neutron stars and black holes e.g. Riles (2013), Cutler and Thorne (2002). Here, we want to investigate whether Gaia can specify the binary fractions for these stellar populations through binary astrometric microlensing. For this goal, we estimate the number of detectable binary events which have considerable binary signals during the Gaia era by performing Monte Carlo simulation according to the Gaia observing strategy.

In the first step, we produce an ensemble of binary astrometric and photometric microlensing events due to massive stellar populations as microlenses according to their physical distributions explained in subsection (3.1). We consider binary stellar-mass black holes, neutron stars, white dwarfs and main-sequence stars as microlenses. Then, corresponding light curves and astrometric trajectories are re-generated according to the Gaia observing strategy. By considering a suitable criterion explained in subsection (3.2), we investigate whether the binary signatures can be inferred from the Gaia observations. Finally, by calculating the optical depth (explained in subsection 2.1), the number of detectable binary events during the Gaia mission are estimated. The results are gathered in subsection (3.2).

3.1. *parameter space*

The distribution functions used to generate the binary astrometric and photometric microlensing events are explained here.

For the source stars, we make an ensemble of the source stars according to their mass, age, metallicity and magnitude and then choose uniformly the source star from that. We take the ages of the stars in the range of $\log(t/yr) = [6.6, 10.2]$ with intervals of $\Delta \log(t) = 0.05$ *dex*. For each age range, we estimate the number of stars according to a positive star formation rate $dN/dt > 0$ (Cignoni et al. 2006; Karami 2010). For each star in this age range, we take the mass of source star, i.e. $M_\star$, from the Kroupa mass function in the range of $M_\star \in [0.1, 3] M_\odot$ (Kroupa et al. 1993; Kroupa 2001) and metallicity, i.e. Z, according to the age−metallicity relation, and the distribution function for the metallicity from Twarog (1980). Finally, we use the theoretical isochrones of the colour−magnitude diagram (CMD) obtained using the numerical simulation of the stellar evolution from the Padova model (Marigo et al. 2008) to simulate the absolute magnitude of each star. The isochrones are defined for stars with different masses, colours and magnitudes but with the same metallicities and ages.

The coordinate of the source star toward the Galactic bulge (l, b, D_s), is selected from $dN/d\Omega \propto \rho(l, b, D_s) D_s^2$ in the range of $l \in [-10, 10]^\circ$, $b \in [-5, 5]^\circ$ and $D_s \in [0, 10]$ *kpc* where $\rho(l, b, D_s)$ is the combination of the stellar densities in the Galactic bulge and disk (Rahal et al. 2009). Galactic bulge has a triaxial structure rotated along the main axes of bulge according to the orientation angles: $\eta = 78.9^\circ$ represents the angle between the bulge major axis and the line perpendicular to the Sun-Galactic center line, $\beta = 3.5^\circ$ is the angle between the bulge plane and the Galactic plane and $\gamma = 91.3^\circ$ is the roll angle around the major axis of bulge (Robin et al. 2003).

We obtain the apparent magnitude of the source star $(m_\star)$ according to the absolute magnitude, distance modulus and extinction. The extinction map towards the Galactic bulge and in the Galactic distance is obtained in some references, e.g. Gonzalez et al. (2012), Nataf et al. (2013). But the extinction map in the closer distances is not clear. We know that the extinction can be determined according to the column density of Hydrogen content of the Galaxy (Weingartner & Draine 2001). The different fractions of Inter Stellar Medium (ISM) in different directions toward the Galactic bulge are due to Hydrogen content. Hence, we need to estimate these fractions in different directions toward the Galactic bulge. We do this by comparing (in the each direction at the Galactic distance) (i) the extinction map provided by Gonzalez et al. (2012) and (ii) the extinction amount calculated according to its relation with the Hydrogen column density by assuming all ISMs are made from the Hydrogen content. We use ISM density law introduced by Robin et al. (2003). Also we obtain the V-band extinction from its value in near infrared bands according to the relations introduced by Cardelli et al. (1989). Indeed, we assume the fraction of ISM composed from the Hydrogen content in the Galactic scale depends only on the direction but not on the distance. The source stars fainter than 20 G magnitudes are not considered.

For generating the light curve of microlensing events with the finite source size effect, we need the radius of source star. For the main-sequence stars, the relation between the mass and radius is given by $R_\star = M_\star^{0.8}$ where all parameters normalized to the sun's value. We do not consider giant source stars. The Gaia astrometric and photometric precisions are pointed out according to the apparent magnitude of source (Varadi et al. 2009). We consider the events in which $\theta_E > 5\sqrt{2}\sigma_a$.

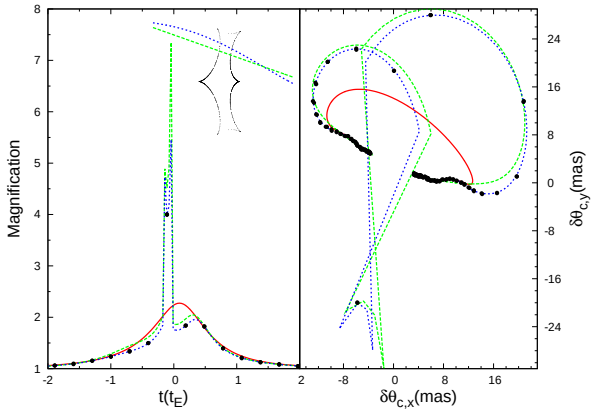

Figure 1. A typical binary microlensing event with binary stellar-mass black holes. The light curves (left panel), astrometric trajectories (right panel) and the source trajectories with respect to the caustic curve (the inset in the left-hand panel) without and with considering the parallax effect are shown with green dashed and blue dotted lines respectively. The point-mass lens models (considering the parallax effect) are shown by red solid lines. Data points taken by Gaia are shown with black points. The relevant parameters of the source and lens are $M_\star = 1.1\ M_\odot$, $m_\star = 15.8\ mag$, $D_s = 2.0\ kpc$, $\xi = -20^\circ$, $v_t = 120\ kms^{-1}$, $u_0 = 0.4$ and $M_l = 10\ M_\odot$, $q = 0.6$, $D_l = 0.4\ kpc$, $d = 0.9\ R_E$ respectively.

For indicating the trajectory of the source with respect to x-axis, we identify this path with an impact parameter and orientation defined by an angle between the trajectory of source star and x-axis i.e. ξ. We let this angle change in the range of $[0, 2\pi]$. The impact parameter is taken uniformly in the range of $u_0 \in [-u_a, u_a]$ and the corresponding time for u_0 is chosen uniformly in the range of $t_0 \in [0, 5]$ years which is the lifetime of Gaia.

To simulate the position of the lens in the Galactic disk, by considering the same Galactic latitude b and longitude l as the source, we take its distance with respect to the observer from the probability function of astrometric microlensing detection $d\Gamma/dx \propto \rho_d(x)(1-x)^2$, where $x = D_l/D_s$ (Dominik & Sahu 2000).

The mass of the stellar-mass black holes as microlenses is taken from the distribution function introduced by Farr et al. (2011). We take the mass of the neutron stars from a Gaussian function, with an average and dispersion of $M_0 = 1.28\ M_\odot$ and $\sigma = 0.28\ M_\odot$ in the range of $[1, 2.5]\ M_\odot$ (Özel et al. 2012). The mass of white dwarfs is taken from a combination of two Gaussian functions with the averages and dispersions of $M_0 = 0.59\ M_\odot$, $\sigma = 0.047\ M_\odot$ and $M_0 = 0.711\ M_\odot$, $\sigma = 0.109\ M_\odot$ for two different samples of white dwarfs in the range of $[0.3, 1.4]\ M_\odot$ (Kepler et al. 2007). We take the mass of main-sequence stars as microlenses from the Kroupa mass function in the range of $[0.1, 2]\ M_\odot$.

The velocities of the lens and the source star are taken from the combination of the global and dispersion velocities of the Galactic disk and bulge (Rahal et al. 2009; Binney & Tremaine 1987).

To simulate the parallax effect, we first convert the Galactic coordinate of the source to the ecliptic coordinate using LAMBDA site[3]. Then, the Earth's position vector with respect to the Sun is calculated (e.g. the Appendix section from An et al. (2002)). The time when the Earth is in the perihelion is $t_e = -18$days with respect to the time when Gaia entered its operational orbit i.e. start time of observation.

Here, we review the Gaia scanning law. Gaia has two astrometric fields of view separated by 106.5°. Its spin axis makes an angle of 45° with respect to the direction towards the Sun. The satellite spins around this axis with the angular rate some of 60 $as\ s^{-1}$. Hence, observations occur in pair whose time interval is 106.5 minutes. The spin axis in turn has a precession motion around a circle. Finally, the spacecraft will move in a Lissajous orbit around the second Lagrange point of the Sun-Earth system. The combination of these motions gives the Gaia scanning law [4]. Each object will be observed 72 times averagely with the cadence some of 25 days. This satellite measures the positions of objects just set along the scan direction. For simulating the observational astrometric trajectories and photometric light curves, we adopt the Gaussian distribution for the cadence between two pairs of data taken by Gaia with the average and dispersion of 25 and 5 days. Each pair occurs in 106.5 minutes. In each observation we consider a random scanning direction chosen uniformly in the range of $[0, 2\pi]$.

Here, we explain distribution functions used for binary systems. For all binary systems we take the mass ratio from the distribution function introduced by Duquennoy & Mayor (1991). We consider binary stellar-mass black holes (BBH), binary neutron stars (BNS), binary white dwarfs (BWD) and binary main-sequence stars (BMS) as microlenses. (Note that, BNS and BWD are not necessarily double neutron stars and double white dwarfs. Their primary lenses are a neutron star and a white dwarf respectively.) We choose the semi-major axis s of the binary orbit from the Öpik's law where the distribution function for the primary-secondary distance is proportional to $\rho(s) = dN/ds \propto s^{-1}$ (Öpik 1924) in the range of $s \in [0.6, 30]\ A.U.$. We use the generalized version of the adaptive contouring algorithm (Dominik 2007) for simulating astrometric trajectories in binary microlensing events.

We let the microlenses rotate around their center of mass. Indeed, the perturbations developed with time such as lens orbital motion can make considerable deviations in astrometric trajectories which helps to discover the second microlens (Sajadian 2014). The parameters of lenses orbit are taken as follows: the time of arriving at the perihelion point of orbit t_p is chosen uniformly in the range of $t_p \in [t_0 - P, t_0 + P]$ where P is the orbital period of lenses motion. The projection angles to specify the orientation of orbit of lenses with respect to the sky plane, i.e. δ and ϑ, are taken uniformly in the range of $[-\frac{\pi}{2}, \frac{\pi}{2}]$. We take the eccentricity of the lenses' orbit uniformly in the range of $e \in [0, 1]$.

3.2. *results*

To determine the detectability of binary signals we calculate χ^2. Two models are fitted to the astrometric and photometric data: (a) the known rotating binary microlensing model with the parameters used to simulate data, i.e. χ^2_b and (b) the simple Paczyński mi-

[3] http://lambda.gsfc.nasa.gov/toolbox/tb-coordconv.cfm

[4] http://sci.esa.int/gaia/40846-galactic-structure

Table 1
The results of the simulation of the binary astrometric microlensing events with GAIA.

	$\overline{t_E}(days)$	$\overline{t_{ae}}(days)$	$\overline{u_a}$	$\varepsilon_b(\%)$	$\Sigma\ (M_\odot\ pc^{-2})$	$\overline{\tau_a}\times 10^{-7}$	$N_b(f=0.1)$	$N_b(f=0.3)$	$N_b(f=0.5)$
BBH	90.2	568.6	18.3	13.5	2.09	8.0	5.6	16.9	28.1
BNS	27.1	109.5	32.8	16.5	0.91	8.6	11.4	34.2	57.1
BWD	17.9	66.0	34.1	15.6	2.41	34.8	76.8	230.3	383.8
BMS	11.5	42.5	43.3	17.6	21.3	434.9	1316.1	3948.4	6580.6

Note. — The average values of the Einstein crossing time $\overline{t_E}(days)$, the duration of the astrometric event $\overline{t_{ae}}$ $(days)$ threshold impact parameter $\overline{u_a}$, efficiency of detecting binary signatures of microlenses $\varepsilon_b(\%)$, the column density $\Sigma\ (M_\odot\ pc^{-2})$, astrometrical optical depth $\overline{\tau_a}$ and number of binary astrometric microlensing events detected with Gaia due to different binary systems: binary stellar-mass black holes (BBH), binary neutron stars (BNS), binary white dwarfs (BWD) and binary main-sequence stars (BMS) considering different binary fractions f.

crolensing events with the same Paczyński parameters, i.e. χ^2_P. Our criterion for detectability of the binary signal is $\Delta\chi^2 = \chi^2_P - \chi^2_b > \Delta\chi^2_{th}$. χ^2_j (for j=b,P) from fitting the astrometric trajectory along the scan θ_s and the magnification factor A is given by:

$$\chi^2_j = \Sigma^N_{i=1}[\frac{(A_i - A_j(t_i))^2}{\sigma^2_A} + \frac{(\theta_{s,i} - \theta_{s,j}(t_i))^2}{\sigma^2_a}] \quad (8)$$

where N is the number of data points and σ_A is the Gaia photometric precision. We assume that from fitting process and searching all parameter space the best-fitted solution is the known binary solution. We consider $\Delta\chi^2_{th} = 200$.

In Figure (1) we show a typical simulated binary microlensing event with binary stellar-mass black holes being observed with Gaia. The light curves (left panel), astrometric trajectories (right panel) and the source trajectories with respect to the caustic curve (the inset in the left-hand panel) without and with considering the parallax effect are shown with green dashed and blue dotted lines respectively. The point-mass lens models are shown by red solid lines. Data points taken by Gaia are shown with black points. The relevant parameters of the source and lens are $M_\star = 1.1\ M_\odot$, $m_\star = 15.8\ mag$, $D_s = 2.0\ kpc$, $\xi = -20^\circ$, $v_t = 120\ kms^{-1}$, $u_0 = 0.4$ and $M_l = 10\ M_\odot$, $q = 0.6$, $D_l = 0.4\ kpc$, $d = 0.9\ R_E$ respectively. In this event, the binary signal is detectable with Gaia. Although, in the photometric light curve there is one data point with significant deviation with respect to the simple microlensing light curves but in the astrometric trajectory there are several deviated data points. Hence, although the Gaia cadence is too sparse so that some of caustic-crossing features may be missed in the photometric light curves but the astrometric measurements can much likely resolve the binary signatures from the second microlenses. Indeed, the astrometric cross section is much larger than the photometric one.

In Table (1) we provide the average values of the Einstein crossing time $\overline{t_E}$, the duration of the astrometric event $\overline{t_{ae}}$, threshold impact parameter $\overline{u_a}$, efficiency for detecting binary signals ε_b, i.e. the fraction of the simulated binary events in which the binary signals are detectable with $\Delta\chi^2 > \Delta\chi^2_{th}$ given in per cent, the column densities for different stellar populations Σ (taken from Flynn et al. (2006) and Chabrier (2001)) and the astrometrical optical depth $\overline{\tau_a}$ from the second to sixth column due to different binary systems. Note that, we calculate the optical depth for different directions toward the Galactic bulge, i.e. l in the range of $[-10, 10]^\circ$ and b in the range of $[-5, 5]^\circ$ and average over all of them.

The expected number of binary microlensing events being observed with Gaia with detectable binary signals, i.e. N_b, is given by:

$$N_b = N_a\ f\ \varepsilon_b, \quad (9)$$

where f is the fraction of binary objects in different stellar populations. To calculate N_a (equation 7) we insert the average values of $\overline{t_E}$, $\overline{u_a}$ for each stellar population. Also, we set the number of background source stars towards the Galactic bulge $N_{bg} = 3.0\times 10^8$ (Caciari 2014). Noting that the number of background stars brighter than 20-G magnitudes for whole sky is on the order of billion objects. The amounts of N_b for three values of $f = 0.1, 0.3$ and 0.5 are reported in Table (1).

According to this table: (i) The Gaia efficiency for detecting different binary systems as microlenses is almost $10 - 20$ per cent which is acceptable according to the sparse cadence of Gaia. It means that Gaia detects the signal from the second lens with probability $\sim 10 - 20$ per cent.

(ii) The Gaia efficiency decreases with increasing the lens mass. Because, by increasing the lens mass, the normalized distance between two lens decreases. Hence, binary black holes usually make close binaries for which the probability of caustic crossing is smaller than that in the intermediate binaries due to the less massive microlenses.

(iii) Gaia can potentially determine the binary fraction of massive stellar populations. Because, the numbers of estimated events for different binary fractions are larger than one. The number of estimated events for binary black holes is small which means that the uncertainty for specifying their binary fraction is high, specially if the real binary fraction would be less than 0.1.

(iv) The duration of the astrometric events is given by (Dominik & Sahu 2000; Belokurov & Evans 2002): $\overline{t_{ae}} = t_E\ \theta_E/(5\sqrt{2}\sigma_a)$ which is proportional to the Einstein crossing time. Indeed, the ratio of $\theta_E/5\sqrt{2}\sigma_a$ is almost constant for different stellar populations and larger than one. Hence, the more massive microlenses with longer Einstein crossing time have the longer astrometric durations. The longest duration of the astrometric

events is that due to binary stellar-mass black holes and some of 1.56 yrs. This time is one third of the Gaia lifetime. The more massive microlenses have longer astrometric duration, comparable with the Gaia lifetime which are not suitable to be observed with Gaia.

4. MEASURING THE MASS OF MASSIVE STELLAR POPULATIONS

Here we investigate how Gaia is efficient to measure the mass of the massive stellar populations through astrometric microlensing of single lenses and specify their mass distributions. In this regard, we quantitatively estimate the Gaia efficiency and the number of high-quality astrometric microlensing events by performing a Monte Carlo simulation.

We consider different stellar populations, i.e. stellar-mass black holes, neutron stars, white dwarfs and main-sequence stars as microlenses and simulate astrometric microlensing events due to these microlenses according to their distribution functions explained in subsection (3.1). Having re-generated the astrometric and photometric curves with synthetic data points according to the Gaia observing strategy, we should indicate whether the lens mass can be inferred from data. In that case, we evaluate the uncertainty in the lens mass i.e. σ_M, in the same way as Belokurov & Evans (2002), and accept the events with the relative error i.e. σ_M/M_l less than 0.5 as high-quality events.

4.1. *results*

The results of this Monte Carlo simulation are summarized in Table (2) which lists the average values of the lens mass $\overline{M_l}$ ($M_\odot$), Einstein crossing time $\overline{t_E}$ ($days$), duration of the astrometric event $\overline{t_{ae}}$ ($days$), threshold impact parameter $\overline{u_a}$, lens-source transverse velocity $\overline{v_t}$ ($km\ s^{-1}$), source distance from the observer $\overline{D_s}$ (kpc), astrometric precision of Gaia $\overline{\sigma_a}$ ($\mu\ as$), efficiency for detecting high-quality events ε (%), i.e. the number of the high-quality events divided by the total number of simulated events given in per cent and finally the number of high-quality events N_e (explained in subsection 2.1) for four different stellar populations.

Interpreting this table: (i) The more massive lenses, the larger efficiencies of measuring the lens mass. Indeed, the Einstein crossing time in astrometric microlensing events due to massive lenses is long. As a result, the number of data over the astrometric trajectories and photometric light curves increases. On the other hand, their angular Einstein radius and astrometric signal are high.

(ii) The Gaia astrometric precision for astrometric microlensing due to more massive microlenses is larger than that due to less massive ones. Indeed, we consider two restrictions for simulating astrometric microlensing events: (a) the source star should be brighter than 20 G magnitude and (b) the angular Einstein radius should be larger than $5\sqrt{2}\sigma_a$. Hence, the average value of σ_a, reported in seventh column, represents the minimum amount of the angular Einstein radius which in turn is an increasing function with respect to the lens mass. As a result, the threshold impact parameter which is proportional to $1/\sqrt{\delta_T}$ decreases with enhancing the lens mass.

(iii) The number of high-quality events due to the massive stellar populations are larger than one. Hence, we can obtain some information about their masses and mass distribution. A significant point is that this method can even give the mass of isolated objects. For the main-sequence stars as microlenses, we conclude that some of 786 high-quality events *toward the Galactic bulge* will probably be confirmed during the Gaia era. However, Belokurov and Evans (2002) estimated that number of high-quality events due to main-sequence stars *for whole sky* is ~ 2500. Indeed, we consider the number of background stars brighter than 20 G magnitudes towards the Galactic bulge as 300 million objects which is so fewer than that was considered by them, i.e. one billion objects. Meantime, there are some differences between the distribution functions used in our simulation and those used in the referred paper. However, they estimated just high-quality events due to main-sequence stars.

Note that the mass ranges of these four stellar populations as microlenses overlap in edges. But, we can discern the type of microlenses with the masses in the common ranges (belong to two populations) through their color and magnitude. Because, these microlenses most likely locate at the distance less than 1 kilo parsec from the observer.

In order to study the dependance of efficiency on the parameters of the model, in Figure (2) we plot the normalized efficiencies, i.e. ε_n, for detecting high-quality events due to stellar-mass black holes (black solid line), neutron stars (red dashed line), white dwarfs (green dotted line) and main-sequence stars (blue dot-dashed line) in terms of the relevant parameters of the lens and source. To compare the efficiency curves with each other, we normalize all efficiency curves to one which means the area under each curve is one, hence we name them as *normalized efficiency curves*. Since the area under each efficiency curve is proportional to the related value reported in the ninth column of Table (2) i.e. ε, the normalization is done by dividing Y values to ε. Generally, the behaviors of efficiency for different stellar populations are similar, although some differences exist in the slope of curves, peak position, etc. The normalized efficiency function in terms of the lens and source parameters is given as follows:

(i) The first one is the impact parameter, u_0. The efficiency of detecting high-quality events is high for astrometric microlensing events with $u_0 < 1$ for which the photometric microlensing can be observed as well as the astrometric one.

(ii) The second parameter is the relative velocity of source with respect to lens, v_t. The efficiency increases with decreasing the relative velocity. Indeed, the Einstein crossing time rises with decreasing the relative velocity. Since the Gaia cadence is almost constant for all events towards the Galactic bulge, so the number of observational data for long-duration microlensing events (over the astrometric trajectories and photometric light curves) is high. As a result, the errors in parameters for these events are smaller than those due to short-duration ones.

(iii) and (iv) Two next parameters: $M_\star$ the mass and $m_\star$ apparent magnitude of source star. The Gaia astrometric precision depends strongly on the source magnitude and increases with decreasing it. Hence, the Gaia efficiency for measuring the lens mass in astrometric microlensing due to brighter and heavier sources is higher

Table 2
The results of the simulation of astrometric microlensing events due to massive stellar populations with GAIA.

	$\overline{M_l}$ $(M_\odot)$	$\overline{t_E}$ $(days)$	$\overline{t_{ae}}$ $(days)$	$\overline{u_a}$	$\overline{v_t}$ $(km\ s^{-1})$	$\overline{D_s}$ (kpc)	$\overline{\sigma_a}$ $(\mu\ as)$	ε (%)	N_e
(BH)	10.3	74.1	460.2	20.1	179.8	4.3	478.8	9.8	44.5
(NS)	1.4	20.5	86.7	29.0	182.5	3.5	324.2	2.9	34.2
(WD)	0.6	12.3	46.6	35.0	182.7	3.1	268.9	1.2	76.3
(MS)	0.4	9.1	33.3	41.0	182.8	2.7	232.1	0.8	785.8

Note. — The average values of the lens mass $\overline{M_l}$ $(M_\odot)$, Einstein crossing time $\overline{t_E}$ $(days)$, duration of the astrometric event $\overline{t_{ae}}$ $(days)$, threshold impact parameter $\overline{u_a}$, lens-source transverse velocity $\overline{v_t}$ $(km\ s^{-1})$, source distance from the observer $\overline{D_s}$ (kpc), astrometric precision of Gaia $\overline{\sigma_a}$ (μas), detection efficiency for high-quality events ε (%) and finally the number of high-quality events being observed during the Gaia era for four different stellar populations: stellar-mass black holes (BH), neutron stars (NS), white dwarfs (WD) and main-sequence stars (MS).

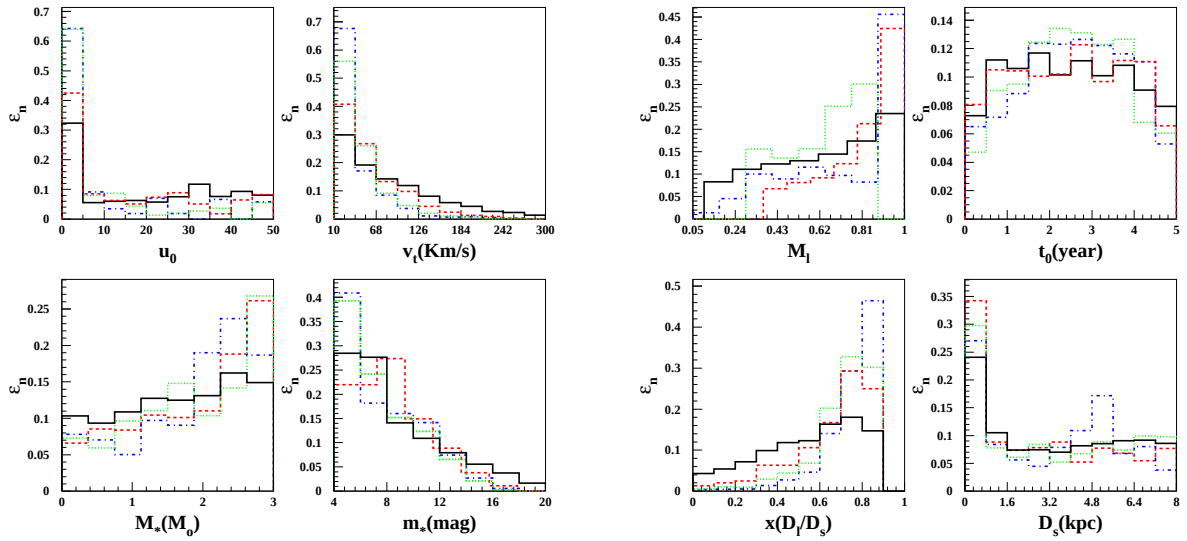

(a) (b)

Figure 2. The normalized efficiency curves, ε_n, of Gaia for measuring the lens mass in astrometric microlensing due to stellar-mass black holes (black solid line), neutron stars (red dashed line), white dwarfs (green dotted line) and main-sequence stars (blue dot-dashed line) for some parameters of source star and lens. Noting that all efficiency curves are normalized to one which means the area under each curve is one, so-called as normalized efficiency curves. Also, the lens mass for each stellar population is divided to its maximum amount so that the range of the normalized lens mass for all populations is in the range of $[0, 1]$.

than that due to fainter and less massive ones.

(v) The next parameter is the normalized lens mass, M_l. Since the mass range for all stellar population is not similar, we normalize the lens mass for each stellar population to its maximum amount so that the range of the normalized lens mass for all populations is in the range of $[0, 1]$. For the massive lenses the Einstein crossing time is long. Consequently, the number of data over the astrometric trajectory and photometric light curve increases. On the other hand, their angular Einstein radius and astrometric signal are high. Therefore, the Gaia efficiency for measuring the mass of more massive lenses is higher than that of less massive lenses.

(vi) The next parameter is the corresponding time to the closest approach, t_0. We uniformly choose t_0 in the range of $[0, 5]T$. But the events with $t_0 \sim 2.5T$ has the maximum efficiency. Because, for these events the number of observational data over the astrometric trajectory and light curve is maximum.

(vii) and (viii) Two last parameters: $x = D_l/D_s$ the relative distance of the lens to the source star from the observer and D_s the source distance from observer. Indeed there are two kinds of suitable sources for the Gaia detection: (a) nearby sources with $D_s < 1\ kpc$ and (b) the bright sources often located at the Galactic disk. Correspondingly, there are two peaks in the efficiency diagram versus D_s. These two classes have the different xs. We know that the Einstein crossing time is proportional to $t_E \propto \sqrt{D_s x(1-x)}$, but the relative parallax and the angular Einstein radius depend on these parameters as $\theta_E \propto \sqrt{\pi_{rel}} \propto \sqrt{\frac{1-x}{D_s x}}$. Although, the efficiency enhances with increasing each of them, but the first is an increasing function versus x and D_s and the others are

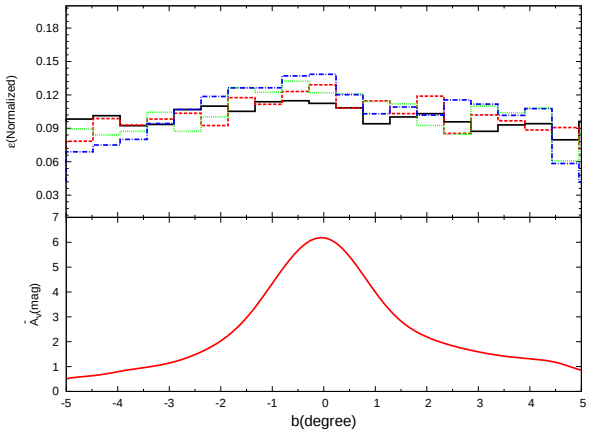

Figure 3. The normalized efficiency of Gaia for measuring the lens mass in astrometric microlensing due to different stellar populations (top panel) and the average value of the extinction in V-band, $\bar{A}_v$, (red solid line) versus the Galactic latitude b. Note that the efficiency curve for each population normalized to the related cumulative value reported in the ninth column of Table 2.

decreasing functions. Therefore, the efficiency is maximized for the first class when $x \sim [0.6, 0.7]$ and for the second class when $x \ll 1$.

According to the dependance of efficiency on the parameters, we expect that most high-quality events have long Einstein crossing times or small impact parameters or their source is a bright star. Hence, most sources are so close to the observer.

We also investigate the dependence of the Gaia (normalized) efficiency on the Galactic latitude, shown in the top panel of Figure (3). The normalized efficiency decreases very slowly by increasing the distance from the Galactic plane. Because, there are two effects act reversely: (i) The extinction toward the Galactic bulge strongly increases by decreasing the distance from the Galactic plane as shown in the bottom panel of Figure (3) and (ii) the Galactic disk density, equation (5), decreases by increasing distance from the Galactic plane. The first effect decreases the probability of finding a source star brighter than 20-G magnitude toward the Galactic center while the abundance of stars is maximum in this direction. Consequently, the efficiency is almost constant over the Galactic bulge. To determine the extinction, we average over the amounts of the extinction due to the Galactic longitudes in the range of $[-10, 10]^\circ$ for each value of b.

5. CONCLUSIONS

One of astronomical phenomena being observed with Gaia is astrometric microlensing events. In this work, we investigated whether Gaia can specify the binary fractions and mass distributions of massive stellar populations through astrometric microlensing.

We simulated binary astrometric microlensing events being observed with Gaia due to binary stellar-mass black holes, binary neutron stars, binary white dwarfs and binary main-sequence stars to evaluate the efficiency for detecting the binary signatures. We considered $\Delta\chi^2 > 200$ as the detectability criterion and concluded that Gaia detects the signal from the second lens with probability $\sim 10 - 20$ per cent. Then, We estimated the number of binary astrometric microlensing due to the mentioned populations with detectable binary signals in the Gaia era as 6, 11, 77 and 1316 respectively ($f = 0.1$). Hence, Gaia can potentially determine the binary fraction of massive stellar populations. Since the predicted number of binary astrometric microlensing events of stellar-mass black holes is small, so the Gaia accuracy to specify their binary fraction is low. The significant points is that binary systems composed of white dwarfs, neutron stars or black holes are sources of detectable gravitational waves. Therefore, indicating the binary fraction of these massive stellar populations helps to assess the amount of the gravitational waves.

Also, we investigated the Gaia efficiency for measuring the mass of massive stellar populations in the Galactic disk, i.e. stellar-mass black holes, neutron stars and white dwarfs in addition to main-sequence stars as microlenses in astrometric microlensing events of single lenses. The Gaia efficiency for measuring the mass of microlenses enhances with increasing the lens mass. By performing Monte Carlo simulation, we concluded that the Gaia efficiencies for detecting high-quality events due to these stellar populations are 9.8, 2.9, 1.2 and 0.8 per cent respectively. We estimated the number of high-quality events for these populations as 45, 34, 76 and 786 respectively. Hence, Gaia can obtain some information about their masses and mass distribution of these massive stellar populations.

I am grateful to Sohrab Rahvar for helpful discussions and comments and Scott Gaudi for careful reading and commenting on the manuscript. I thank anonymous referee for useful comments and suggestions which certainly improved the manuscript. Also, I acknowledge the use of the Legacy Archive for Microwave Background Data Analysis (LAMBDA), part of the High Energy Astrophysics Science Archive Center (HEASARC).

REFERENCES

An J.H., Albrow M.D., Beaulieu J.-P, et al., 2002, ApJ, 572, L521.
Belokurov, V. A. & Evans, N. W., 2002, MNRAS 331, L649.
Belokurov, V. A. & Evans, N. W., 2003, MNRAS 341, L569.
Binney, S., & Tremaine, S. 1987, Galactic Dynamics (Princeton, NJ: Princeton Univ. Press), 78.
Boutreux T., Gould A., 1996, ApJ, 462, L705
Cacciari C., 2014, Proc. of the workshop, (arXiv:1409.2280)
Cardelli J. A., Clayton G. C. & Mathis J. S., 1989, ApJ, 345, L245.
Chabrier, G., 2001, ApJ, 554, L1274.
Cignoni M., Degl'Innocenti S., Prada Moroni P.G. & Shore S. N., 2006, A& A, 459, L783.
Cutler C. & Thorne K. S., 2002, (arXiv:gr-qc/0204090v1).
Dominik M., 2007, MNRAS, 377, L1679.
Dominik M. & Sahu K. C., 2000, ApJ, 534, L213.
Duquennoy A. & Mayor M., 1991, A & A, 248, L485.
Einstein A., 1936, Science, 84, L506.
Eyer L., Holl B., Pourbaix D., et al., 2013, CEAB, 37, L115.
Farr W. M., Sravan N., Cantrell A., et al., 2010, ApJ, 741, L103.
Flynn, C., Holmberg, J., Portinari, L., Fuchs, B., & Jahreiß, H., 2006, MNRAS, 372, L1149.
Gonzalez O. A., Rejkuba M., Zoccali M., et al., 2012, A & A, 543, L13.
Gaudi B. S., & Bloom, J. S., 2005, ApJ, 635, L711.
Høg, E., Novikov, I. D., & Polnarev, A. G. 1995, A & A , 294, L287.
Jeong Y., Han C. & Park S.-H. 1999, ApJ, 511, L569.
Karami M., 2010, MSc thesis, Sharif Univ. of Technology.

Kepler, S. O., Kleinman S.J., Nitta A., et al., 2007, MNRAS, 375, L1315.
Kroupa, P., Tout, C. A., & Gilmore, G. 1993, MNRAS, 262, L545.
Kroupa, P. 2001, MNRAS, 322, L231.
Marigo P., Girardi L., Bressan A., Groenewegen M. A. T., Silva L. & Granato G. L., 2008, A & A, 482, L883.
Miralda-Escudé J., 1996, ApJ, 470, L113.
Miyamoto, M. & Yoshii, Y. 1995, AJ, 110, L1427.
Nataf D. M., Gould A., Fouqué P., et al., 2013, ApJ, 769, L88.
Öpik, E., 1924, Pulications de. L'Observatoire Astronomique de I'Université de Tartu, 25, L6.
Özel, F., Psaltis, D., Narayan, R. & Villarreal A. S., 2012, ApJ, 757, L55.
Paczyński B., 1996, Acta Astron., 46, L291.
Paczyński B., 1998, ApJ, 494, L23.
Proft A., Demleitner M. & Wambsganss J., 2011, A & A, 536, L50.
Rahal, Y. R., Afonso C., Albert J.-N., et al. 2009, A & A, 500, L1027.
Riles, K., 2013, PrPNP, 68, L1.
Robin, A. C., Reylé, C., Derrière, S., Picaud, S., 2003, A & A, 409, L523.
Sajadian, S., 2014, MNRAS, 439, L3007.
Twarog B. A., 1980, ApJS, 44, L1.
Varadi, M. Eyer, L., Jordan, S., Mowlavi, N. & Koester, D. 2009, AIPC 1170, L330.
Walker M. A. 1995, ApJ, 453, L37.
Weingartner, J. C.& Draine, B. T. 2001, ApJ 548, L296.